IEEE Access
Multidisciplinary | Rapid Review | Open Access Journal

Received March 9, 2020, accepted March 20, 2020, date of publication March 24, 2020, date of current version April 7, 2020.

Digital Object Identifier 10.1109/ACCESS.2020.2982965

Wearable Antennas for Cross-Body Communication and Human Activity Recognition

WENJING SU[1,2], (Member, IEEE), JIANG ZHU[1], (Senior Member, IEEE), HUAN LIAO[1], AND MANOS M. TENTZERIS[2], (Fellow, IEEE)

[1]Google LLC, Mountain View, CA 94043, USA
[2]School of Electrical and Computer Engineering, Georgia Institute of Technology, Atlanta, GA 30332, USA

Corresponding authors: Jiang Zhu (jiangzhu@ieee.org) and Wenjing Su (wenjing.su.gatech@gmail.com)

This work was supported by the Google Internship Program.

ABSTRACT This paper proposes a novel miniaturized wearable antenna (mosaic antenna) for cross-body communication featuring a superior performance compared to five commonly utilized wearable antenna topologies. The proposed mosaic antenna optimally excites the surface waves to enable cross-body communication yet still with a low profile and a miniaturized size. As a proof-of-concept of the unique capabilities of this antenna, an inkjet-printed flexible wearable prototype on Polytetrafluoroethylene (PTFE, also known as Teflon) has been fabricated in a highly customizable, scalable and low-cost process and has been used as an enabler for human activities recognition coupled with machine learning techniques powered by Google TensorFlow. By utilizing proof-of-concept on-body networks consisting of mosaic antennas, human activity can be detected with an accuracy 91.9% for RF signal-based recognition techniques, despite the variability among different users and environments.

INDEX TERMS Additive manufacturing, flexible antenna, human activity recognition, machine learning, minimized antennas, wearable antennas.

I. INTRODUCTION

As the wearable electronics industry is growing dramatically every year, novel mind-blowing wearable products have been seen in the market over the last decade. Meanwhile, academic research effort in wearable electronics has been growing tremendously every year [1]. The ''smart'' features of most wearable electronics highly rely on wireless communication systems [2]–[4], in which wearable antenna design is one of the major challenges and requires a special attention [5], [6]. Wearable antennas suffer performance decrements from detrimental human body proximity effects, namely detuning, attenuation and shadowing effects, due to the high-permittivity and high-loss dielectric properties of the human body [7], [8]. The most comprehensive problem is the shadowing effect: the body is commonly in the line of sight (LOS) between transmitters and receivers, thus preventing a high-quality LOS communication. In this case, the utilization of surface waves is one of the best solutions, which is independent of the environment, and thus very reliable [9], [10]. Moreover, to achieve a compact device size and a comfortable wearing experience, reducing the size of the wearable antenna is a crucial but challenging task as the antenna efficiency and impedance are largely related on its physical size comparing to the wavelength. Researchers have been extensively studying the on-body performance of various novel low-profile miniaturized wearable antenna topologies to overcome both body effects and minimization requirements [5], [11]–[16]. This work compares several widely utilized wearable antennas in terms of performance under the above three body effects and introduces a novel metamaterial-inspired antenna, mosaic antenna, featuring 90% height reduction compared to the monopole antenna, 80% area reduction compared to the patch antenna, and excellent excitation of the surface waves.

Given the dynamic nature of human body, the wearable antennas need to be flexible and have a stable performance under different bending and flexing conditions [17]. Fabric and conducting thread is the most straight-forward solution for wearable antennas [18]–[21], as it can be easily embedded into clothes. However, due to its porous thread nature, the bulk conductivity of textile antennas is relatively

The associate editor coordinating the review of this manuscript and approving it for publication was Guido Valerio.

low and their performance at higher frequencies can be unreliable. Stretchable conductors, such as liquid metal and graphene, and stretchable polymers, such as polydimethylsiloxane (PDMS), also have enabled novel stretchable wearable antennas [2], [22]–[24], although the cost handling of these materials still poses numerous problems. Printing on flexible substrates features relatively high conductivity, low dielectric loss, low cost, high speed, maturity and massive scalability, thus being one of the best candidates for the manufacturing of wearable [3], [5], [25], [26]. This paper introduces the first reported inkjet printing of wearable antennas on bio-compatible PTFE (Polytetrafluoroethylene, also known as Teflon) substrate.

Due to the body effects along with flexibility and size constraints, wearable antennas often become one of the most limiting factors in body area networks (BAN) communications, while they could simultaneously function as wearable sensors for motion tracking and human activity recognition (HAR). HAR is a key enabler of numerous state-of-the-art techniques including virtual reality (VR) and augmented reality (AR), and has been widely used in fitness, medical treatment, entertainment, and military. Typically, HAR/human motions tracking is realized using external cameras or body-area sensing networks. External cameras often have difficulties in tracking body motion in moving scenario, such as walking or running, while body-area sensor networks can solve the problem. In the body-area sensor networks, no matter what sensors are used, wearable antennas are an unavoidable components to enable wireless communication [27]. That is why we propose a novel and versatile way to take advantage of received signal strength indicator (RSSI) of the proposed mosaic wearable antennas to effectively monitor body motions and detect human activities. This solution is compatible with the existing body area sensor solutions with no extra element needed, and it can work both with and without other wearable sensors. Taking advantage of the proposed solely RSSI-based approach, a good accuracy of HAR can be easily achieved after using machine learning techniques to process the raw data.

II. WEARABLE ANTENNA DESIGN

A. WEARABLE ANTENNA

As one of the most important elements in communication systems and probably the one that is most heavily influenced by the ambient environment, antennas for wearable applications can significantly affect the system performance. Though the unwanted body effects are unavoidable, their detrimental effects on different antenna structures can have huge differences. This work aims to design a minimized antenna for on-body communications that can fit in compact wearable devices and can drastically outperform commonly used planar antenna topologies, namely monopole antenna, patch antenna, dipole antenna, Inverted-F antenna (IFA), and slot antenna that are shown in Fig. 1(a)-(e), which all operate at 2.4 GHz spectrum for bluetooth (BT) and bluetooth low energy (BLE), the most commonly used wireless protocol for BAN. The impact of the body effects on these five commonly used antennas are shown in Fig. 1(f)-(i). The detuning effect is referred to shift of the antenna's resonant frequency when placed proximity to high-permittivity materials, such as the human body. Moreover, due to the high dielectric loss of human body, the radiation efficiency of the antenna often decreases when placed close to the human body, which is known as attenuation effect. Fig. 1(f)&(g) clearly demonstrates that the most antenna structures are strongly affected by the detuning and the attenuation effects, while the three antennas without a ground plane (dipole, slot, and IFA antennas) shows a much more drastic frequency shift and attenuation, which leads to the rather simple conclusion that ground plane or proper isolation is beneficial to wearable antennas.

The shadowing effect is much more complicated as it is the result of the human body obstructing the line-of-sight (LoS) between transmitters and receivers, which frequently happens in the on-body networks. One way to resolve this issue is utilizing the multipath effect in a reflection-rich environment, for example, the waves can be reflected/scattered to numerous directions by walls and furnitures inside a small room. However, this environment-dependent approach can be extremely unreliable in outdoor or other open environments. In this case, an antenna that can maximally excite surface waves can provide reliable BAN communication even in the worst case scenario [9], [10]. Fig. 1(h) emulates the cross-body performances with various antennas and particularly, Fig. 1(i) shows the cross-head. Compared to the monopole antenna, the patch antenna in a vertical orientation features an S21 that is at least 5 dB worse (Fig. 1(h)&(i)), while their efficiency only features a 3.5 dB difference (Fig. 1(g)). Moreover, the patch antenna is orientation sensitive: in Fig. 1(h), a larger than 20 dB difference in the path loss between the horizontal and the vertical orientation suggests that the patch antennas can only successfully excite the surface waves in certain directions. Interestingly, the patch antenna features a worse performance in vertical orientation and a better performance in vertical orientation in Fig. 1(i), due to the increased complexity of the shape of the realistic head phantom (compared to the simplistic rectangular phantom in Fig. 1(h)), which also demonstrates the significance of orientation-independent antenna performance as the shape of the human body is rather complex. The other commonly used wearable antennas discussed in this paper (the dipole, the slot and the IFA antennas) feature 16 to 35 dB worse S21 values comparing to a testing monopole antenna in proximity to a phantom (Fig. 1(h)) and 2 to 15 dB lower efficiency (Fig. 1(g)) in both orientations, which demonstrates that, excluding efficiency degradation, monopole antenna's capability in exciting surface waves for on-body communication is still outstanding and unbeatable. This is due to the fact that the monopole antenna on the phantom can largely generate a TM mode electrical field that features a better performance in exciting surface waves, thus enhancing on-body transmission [9].

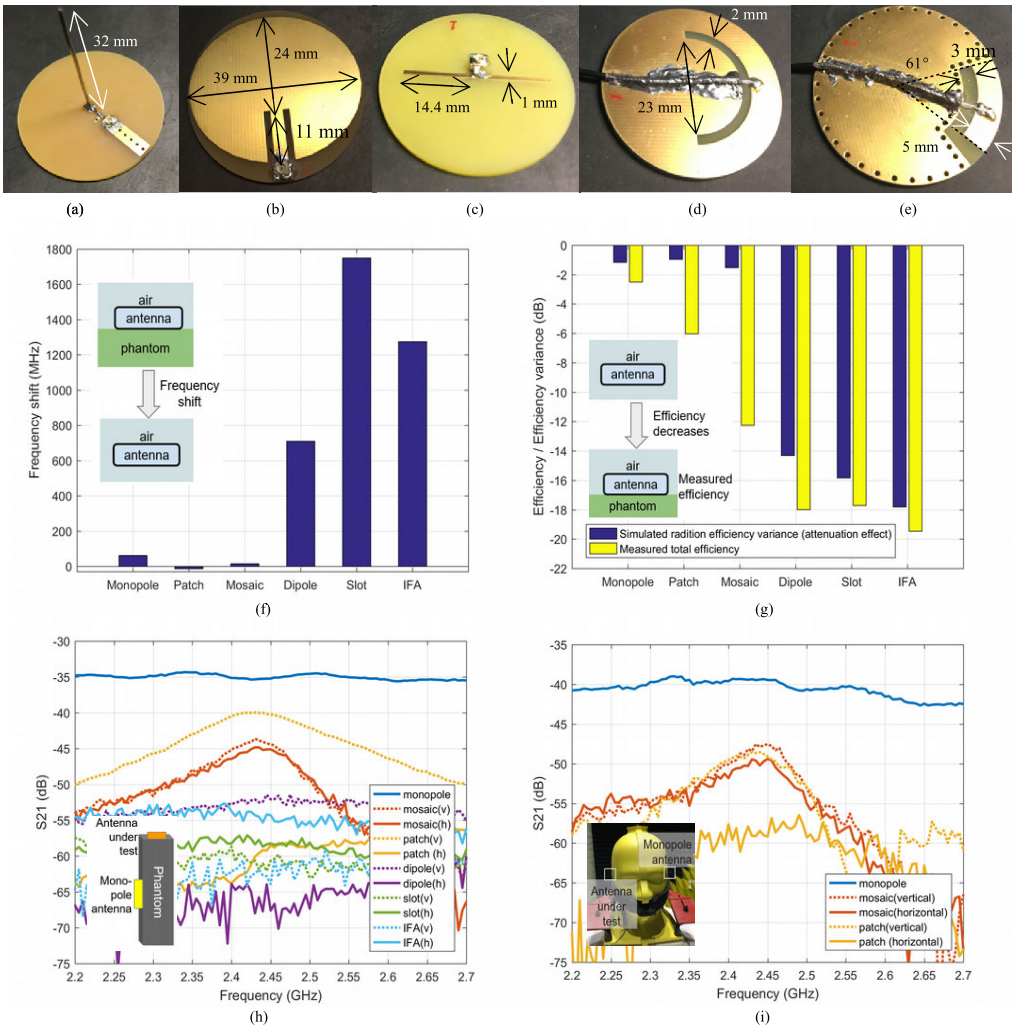

FIGURE 1. **Comparison of the on-body performance of five commonly used antennas and the proposed novel mosaic antenna. Photos of prototypes of (a) the monopole antenna, (b) the patch antenna, (c) the dipole antenna, (d) the slot antenna, (e) the inverted-F antenna. (f) the measured resonant frequency shift of the antenna changing from an on-body (phantom) scenario to free space (air) in the configurations shown in the inserted graph, showing the detuning effect. (g) simulated radiation efficiency decrease (attenuation) from free space to on-body (phantom) scenaria in blue, along with the measured total efficiency of the antenna on phantom in yellow, demonstrating the attenuation effect due to the human body. (h) measured S21 between a monopole antenna (the fixed testing antenna) and the antenna under test (one of the six above-mentioned antennas) when the two antennas are placed in the center of two adjacent faces of the rectangular phantom as shown in the inserted graph in two orientations, 'h' for horizontal and 'v' for vertical, demonstrating the transmission attenuation of different antennas in a scenario that surface waves dominate. (i) measured S21 between a monopole testing antenna and the antenna under test (monopole antenna, patch antenna, or mosaic antenna) when the two antennas are placed on the two ears of the head phantom as shown in the inserted photo for two different orientations, to imitate a typical communication around the head, such as that between two wireless earbuds.**

All the S parameter and efficiency measurements are done in an anechoic chamber with a Vector Network Analyzers (VNA). The rectangular shape phantom used in Fig. 1(f)-(h) is speag BLAP-V1, featuring permittivity of 25.7 and conductivity of 1.32 S/m to mimic lap tissue, and the head shape phantom in Fig. 1(i) is speag SAM-V4.5BS, featuring permittivity of 39.2 and conductivity of 1.8 S/m.

B. MOSAIC ANTENNA

Though the monopole antenna features a minor detuning effect, a minor attenuation effect, and the best surface waves excitation in all directions to overcome shadowing effect, it is still not considered as a good wearable antenna, due to its high profile that prevents most practical on-body applications, such as in ''smart skins''. Moreover, a compact size is extremely significant in numerous wearable devices, such as watches, earbuds, and glasses, that pose very strict size limitations. Therefore, this paper proposes a meta-material inspired antenna, Mosaic antenna, as shown in Fig. 2(a)&(e), which features a similar performance to the monopole antenna, while it is planar and miniaturized.

The mosaic antenna is based on the unit cell shown in Fig. 2(b), which consists of a transmission line, a shunt inductor that could be in the form of lumped element or

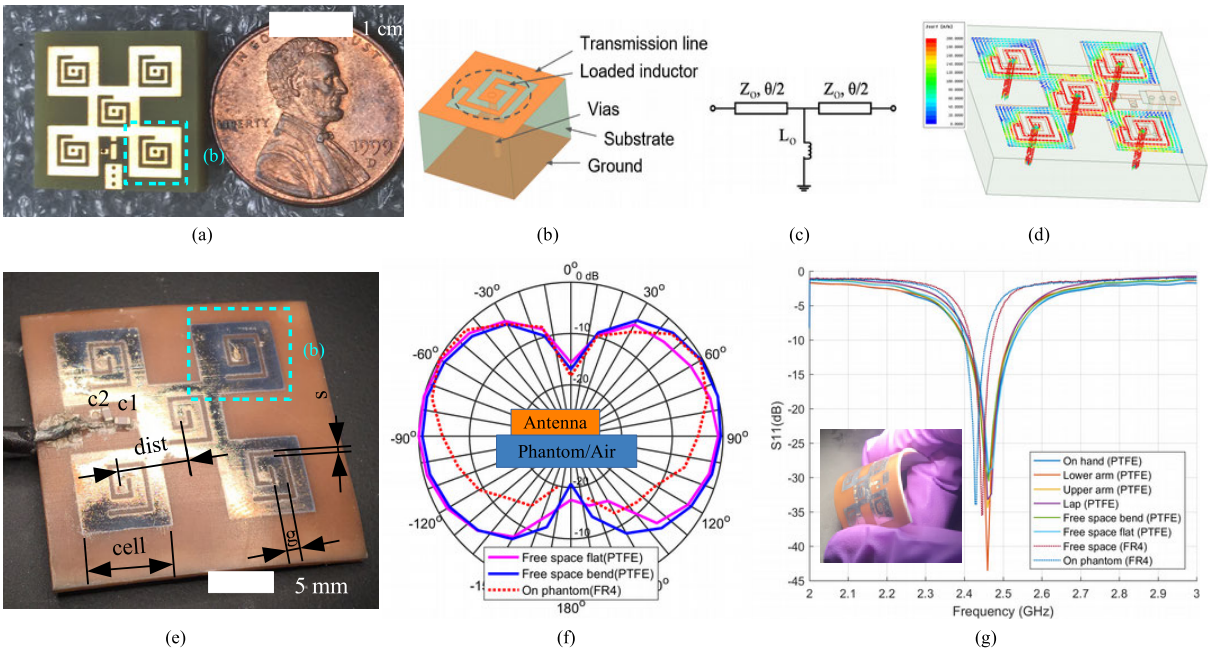

FIGURE 2. Mosaic antennas and their performance. Photo of (a) the rigid mosaic antenna on FR4 substrate, (e) the flexible mosaic antenna on PTFE substrate. (b) the structure of unit cell of the mosaic antennas shown in (a) and (e). (c) equivalent circuit of the unit cell in (b). (d) simulated surface current distribution of the mosaic antenna, showing an in-phase and similar magnitude of current distribution in each cell. (f) measured radiation patterns of the flexible mosaic antenna in flat and bending (radius=27 mm) configurations in free space and of the rigid mosaic antenna on the phantom. (g) the measured S11 of the flexible mosaic antenna for different on-body positions of the body and bending (radius=27 mm) or flat in free space along with the measured S11 of the rigid mosaic antenna on phantom and in free space. The inserted photo in (g) shows bending of the mosaic antenna (PTFE) with two fingers to a radius of 15 mm, showing an excellent flexibility.

printed element, and is implemented as a spiral coil as a proof of the concept, and a via connecting the inductor to the ground plane [28]. The loading inductance is carefully selected so that the structure features a zeroth order resonance near the operating frequency [28] while an L-shaped matching network which consists of two capacitors is exploited to match the impedance to 50 Ohm as shown in the S11 plot in Fig. 2(g). Fig. 2(c) shows the equivalent circuit of a unit cell of the mosaic antenna, which could be as small as 5 mm by 5 mm at the operating frequency 2.4 GHz, or $\lambda/13$ by $\lambda/13$. Transmission-line metamaterials have long been used for antenna's miniaturization [28]–[30]. Here, the metamaterial inspired structure features similar magnitude in-phase current values when fed through the center cell, as shown in Fig. 2(f), which ensures a folded-monopole radiation pattern [31] similar to the radiation pattern from a regular monopole antenna as shown in Fig. 2(g). A proof-of-concept mosaic antenna topology is exploited throughout the paper which consists of only 5 unit cells to significant reduce the antenna size while maintaining a reasonable antenna efficiency. A "X-shape" topology ensures a rotational symmetrical radiation pattern which is desired for robust cross-body wireless communication. The impedance of the mosaic antenna is matched to 50Ω with a series capacitor and a shunt capacitor However, the mosaic antenna, like mosaic arts, can take advantage of any number (>1) of unit cells and any different topology as required by different specifications.

In order to compare with the other commonly utilized on-body antennas discussed in the previous section, a mosaic antenna prototype is designed on a 3-mm-thick FR4 substrate, featuring 90% height reduction compared to the monopole antenna and 80% area reduction compared to patch antenna. The overall size of the mosaic antenna is comparable to an 1-cent coin as shown in Fig. 2(a). In comparison to the other antennas, a frequency detuning as small as 16 MHz and an efficiency reduction as small as 1.5 dB can be observed in Fig. 1(f)&(g), which demonstrates a better or equally good performance. The resulted efficiency of the mosaic is relatively low due to the small antenna aperture size compared to commonly used antennas. In Fig. 1(h)&(i), S21 values of the mosaic antenna in both orientations are around 10 dB less than the monopole antenna, which is exactly the same as the radiation efficiency difference between the two antennas. Due to its orientation-independence and the excellent surface waves excitation capability in Fig. 1(i), the mosaic antenna features a similar or better performance comparing to the patch antenna, even though the radiation efficiency of the mosaic antenna is more than 6 dB lower than the patch antenna.

All the seven antennas in this paper are designed and optimized with Ansoft HFSS, a 3D full-wave finite element method (FEM) simulator. The on-body simulation in Fig. 1(g) uses the data of the rectangular phantom with permittivity of 25.7 and conductivity of 1.32 S/m. In order to compare

TABLE 1. Dimensions of the two mosaic antenna prototypes (Unit: mm) and values of the matching lump capactors (Unit: pF).

Name	FR4	PTFE	Name	FR4	PTFE
Substrate thickness (mm)	3	0.79375	s (mm)	0.4	0.5
Vias diameter (mm)	0.2	0.2	g (mm)	0.3	1
Ground plane width/length (mm)	16	23.6	c1 (pF)	0.75	0.8
dist (mm)	4	6.3	c2 (pF)	1.5	0.3
cell (mm)	5	7.6			

all conventional antennas in Fig. 1(a)-(e) in the same operation/implementation scenario, the antenna prototypes were designed on a 40-mm-diameter 1.5-mm-thick FR4 substrate and operated at 2.4 GHz Bluetooth bands. The FR4 substrate features relative permittivity of 4.4 and dielectric loss tangent of 0.02 while PTFE substrate features relative permittivity of 2.2 and dielectric loss tangent of 0.002.

C. FLEXIBLE ANTENNA

Another challenge in the design of wearable antennas is the necessity of flexible implementations with only minor performance degradation under bent conditions, as large rigid antennas would be especially uncomfortable to wear. Besides the rigid FR4 mosaic antenna prototype for comparison (Fig. 2(a)), a similar mosaic antenna is designed on 0.762-mm-thick PTFE, a flexible substrate. PTFE is biocompatible and widely used in wearable applications, which also features an extremely low cost and various thickness available in the market. However, PTFE is not one of the most frequently used substrates due to its poor wettability [32]. Thus, proper surface treatment is needed to improve the surface energy of deposited solvent-based inks [33]. Inkjet printing silver nanoparticles ink was used to deposit a thin and flexible layer of conductive pattern. The vias were drilled on the PTFE substrate and were filled with high-conductivity silver paste. The fabricated antenna is shown in Fig. 2(e) and is bent easily with two fingers and 15-mm bending radius, as shown in the inserted photo in Fig. 2(g). However, the surface mounted capacitors limit the reliable bending radius so the measurement is done at 27-mm bending radius. This problem can be easily resolved by eliminating the use of the lumped elements and using other matching methods, such as meander line inductor matching [28].

Fig. 2(f) shows the radiation patterns of the rigid FR4 mosaic antenna on phantom as well as of the flexible PTFE mosaic antenna in flat and bending configuration with a 27-mm bending radius. In Fig. 2(f) the radiation pattern in bending was measured by taping the flexible mosaic antenna to a foam cup with 27 mm radius. On-body S11 measurement in Fig. 2(g) was conducted by taping the flexible mosaic antenna at different positions on the body. These specific positions were chosen as same in the HAR experiments. The flat and bending results are very similar with a minior difference to the direction of the ground of the antenna, which is expected as the antenna was conformally attached to a foam cylinder using its ground side. The reduction in the lower half plane radiation of the FR4 mosaic antenna is due to the high loss and high dielectric constant of the phantom. Fig. 2(g) shows the return loss of the rigid FR4 mosaic antenna and and of the flexible PTFE mosaic antenna in different scenarios. Less than 10MHz (0.4%) frequency detuning with an excellent impedance matching (S11<-25 dB) can be observed for the flexible antennas that have been conformally attached to four different areas of the human body, including hand, upper arm, lower arm, and lap, and in flat and bent in-air configurations, which demonstrates a stable on-body performance. The narrow bandwidth of the proposed is due to the thin substrate thickness, which is an unavoidable constraint of wearable antennas.

All the inkjet printing was conducted in a Dimatix DMP-2831 inkjet printer (Fujifilm Dimatix, Inc., Santa Clara, USA) with a 1.5-mL-capacity cartridge which had a 10 pl drop volume (DMC-11610, Fujifilm Dimatix, Inc.). A 20 μm drop spacing and 30 °C platform temperature were chosen to balance the printing speed and performance. The silver nanoparticle ink used is Suntronic Jet Silver EMD5730 from Sun Chemical Corporation (Parsippany, USA). After 4 layers of printing, the ink was sintering at 180 °C for 1 hour and achieve a sheet resistance of 0.02 Ω/square. The PTFE substrate is adhesive-back PTFE sheet from McMASTER-CARR, but alternatively can be any PTFE substrate with surface modification [34]. Before printing, the adhesive layer of the purchased PTFE substrate was removed by acetone bath to reveal the pre-treated wettable PTFE surface.

III. HUMAN ACTIVITY RECOGNITION APPLICATION

A. HAR SYSTEM

The proposed wearable antenna could be especially useful in accurate and real-time body motion tracking and human activity recognition (HAR) systems. Though numerous methods, including optical camera, gyroscopes sensors, and mechanical exoskeleton systems, have been proposed for the implementation of HAR systems, the proposed radio frequency (RF) wireless approach distinguishes itself by its inherently versatile feature that it can take advantage of the sensing capabilities of the on-body sensor network without compromising its original communication functionality. Meanwhile, all on-body sensor networks need wireless communication [27] and this method can be a great add-on to the existed HAR sensing systems virtually for no cost. Unlike visual based tracking, this approach works great for outdoor and moving scenarios, such as jogging and walking, in which environment varies but features less reflections. However, due to the excellent surface waves excitation capability, this RF signal based approach can also be used in the indoor scenario as discussed below.

The inserted graph in Fig. 3(a) shows a proof-of-concept on-body network: several BLE beacons with mosaic antenna are attached to different parts of the body, working as sensor nodes and transmitters, and a cell phone is fixed on the head similar to the VR configuration, working as a data processor

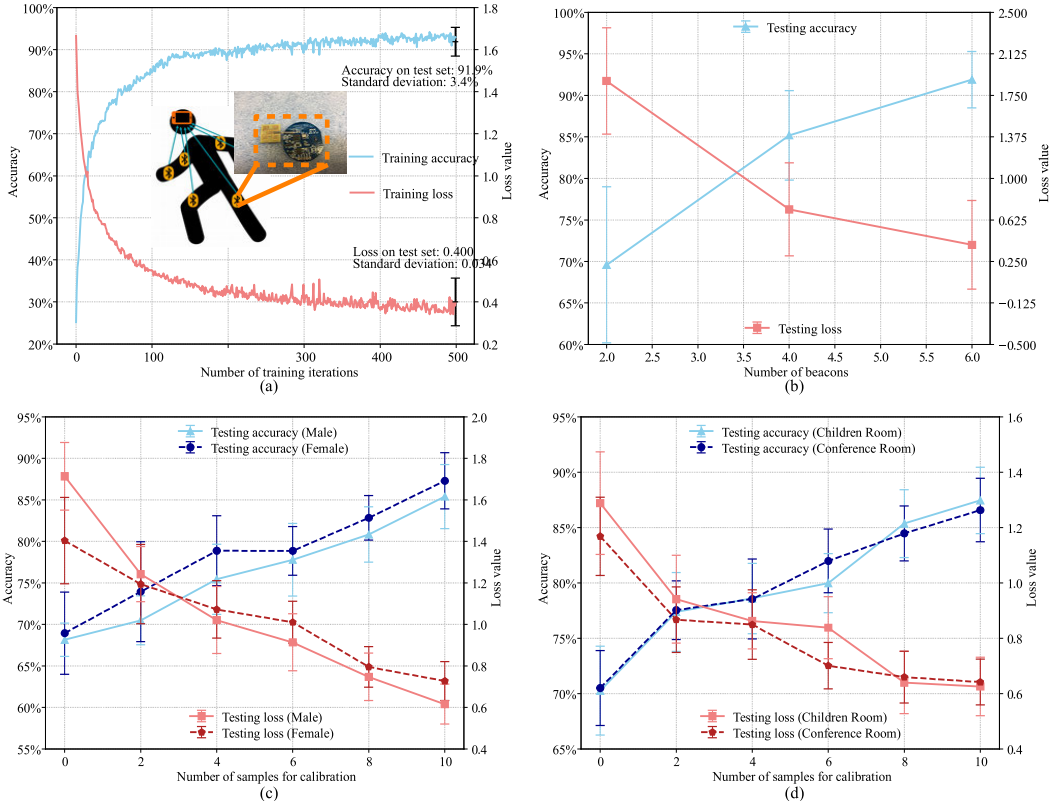

FIGURE 3. Motion tracking and human activity recognition (HAR) performance of a proof-of-concept mosaic-antenna-enabled wireless HAR system. (a) Overall accuracy and loss value of the HAR at increasing training iteration numbers along with an inserted graph indicating the locations of beacons and a photo of the BLE beacon with the mosaic antenna. (b) Accuracy and loss value of the HAR for different numbers of beacons. (c) Accuracy and loss value of the HAR for two new users (one male and one female) for different numbers of samples used in training to calibrate the system. (d) Accuracy and loss value of the HAR for two different locations for different number of samples used in training to calibrate the system.

and as a receiver gateway. The sensor positions chosen feature a large change in their relative location during human activities while they are far from the joints to avoid uncomfortable wearing experience. The received signal strength indicator/index (RSSI) values of the onbody sensor nodes can be collected on the cellphone on-the-fly and analyzed to identify the activity being performed. In the proposed method, the inputs are sequences of RSSI from each sensor while the action is being performed and the output is the label of the action, which is a classical multivariate time-series classification problem, which is best suited for machine learning techniques, in particular, recurrent neural networks (RNNs). Among the most recent developments of RNN models, Long Short-Term Memory (LSTM) cells is the state-of-the-art and is chosen in this paper, and the implementation is based on TensorFlow, a robust deep learning framework from Google that has been proven successful with many industrial-strength applications.

The beacons in this work is based on a Dialog Semiconductor's Bluetooth Low Energy (BLE) 4.2 SOC DA14580. Its conducted power is 0 dBm, which is well below the specific absorption rate (SAR) test exclusion threshold from Federal Communications Commission (FCC). Therefore, it is complied with the RF regulations on electromagnetic exposure on human body. An in-house app is developed for measuring and recording signal strengths specifically for attached beacons. The app leverages the official Core Bluetooth framework which provides the Bluetooth LE peripheral device discovery and signals measurement capabilities. The app can providing accurate received signal strength indicator/index (RSSI) in the range of 0 to -100 dBm at the rate of approximately 10 data points per second per beacon in an energy efficient manner.

B. NEURAL NETWORK PROCESSING

Though RSSI can represent attenuation/distance of the signal pathway, due to the complexity of the shape of the human body as well as the surrounding environment and Bluetooth frequency hopping characteristics, the variance of RSSI data can be hard to interpret. In this paper, we use a Recurrent Neural Network (RNN) with Long Short-Term Memory cells (LSTMs) as the learning architecture. RNN-based machine learning has demonstrated promising performance

results in many similar applications that involve multivariate time-series data, including speech recognition [35], video processing [36], and many other sequence labeling tasks [37]. The rationale behind is RNN's ability to encode contextual information and learn the temporal dependencies in input data. The RSSI value can be fed directly into the neural network which acts like a black box in a high level and is able to model the problem correctly. LSTM has been proven useful in various kinds of HAR applications such as [38]–[40], due to its effectiveness in capturing useful patterns of previous observations, providing longer-range context for the current classification, and processing time series when there can be long time lags of unknown size between important events. Although several other methods have been proposed in the literature of HAR using machine learning techniques [41], the performance (i.e., classification accuracy) of such methods largely depends on the feature extraction, and typically hand-crafted features derived from domain knowledge is required to ensure a good performance. Compared with these methods, the LSTM-based technique used in this paper requires no feature engineering. Compared to dynamic time warping (DTW) [42], LSTM features a much better capability to handle complex relations. Compared to deep convolutional neural networks [43], LSTM is essentially better for processing time sequence information and no preparation processing is needed. A LSTM memory cell contains more parameters and gate units compared with a neuron in traditional RNNs. A typical LSTM cell consists of four main elements: an input gate, a neuron with a self-recurrent connection, a forget gate, and an output gate. The self-recurrent connection ensures that, barring any outside interference, the state of a memory cell can remain constant from one-time step to another. The gates serve to modulate the interactions between the memory cell itself and its environment. The input gate can allow incoming signal to alter the state of the memory cell or block it. On the other hand, the output gate can allow the state of the memory cell to have an effect on other neurons or prevent it. Finally, the forget gate can modulate the memory cell's self-recurrent connection, allowing the cell to remember or forget its previous state, as needed.

C. HAR PERFORMANCE TEST

In order to test the proof-of-concept HAR system that is based on a wireless on-body network, two females and two males perform the five activity(''stand'',''walk'', ''sit'', ''right jab'', and ''left jab'') in three different rooms (activity room, children room, and conference room) for a total of 1200 samples. All activities are recorded as 5 s RSSI sequences, in which ''walk'' is a continuous activity at user's comfortable speed, while the other activities are only performed once at user's comfortable speed, starting from ''stand'' before the action and back to ''stand'' after the action. In order to obtain representative data, all training data and test data were randomly chosen for each tests and all tests were performed for 20 times to enable a sufficiently accurate calculation of both average values and standard deviations.

The test of the proposed HAR system results in Fig. 3(a), showing an overall accuracy at 91.9% with 3.4% standard deviation and a loss of 0.4 with a 0.034 standard deviation after 500 training iterations. The loss value here shows the actual cost function used by the LSTM-based neural network. Compared with using the intuitive ''accuracy'' as the cost function for the neural network, a cross entropy loss reflects not only how good the model can make predictions, but also how good the model can distinguish among the labels. Fig. 3(b) shows that the accuracy increases largely when the number of beacons increases, but the accuracy wouldn't always increases as the number of beacons increases. Two beacons on the lower arms are used for the 2-beacon configuration while all four beacons on the arms are used for 4-beacon configuration. As mentioned above, the system is sensitive to new users and different environments as the dominant signal path may change and scattering from the surrounding objects may bring unwanted interference. As expected, the accuracy decreases when calibration data is not sufficient for a new user or a new location, as shown in Fig. 3(c)&(d). With 10 calibration samples for each activity for new users or new locations, the accuracy is increased to more than 85% from around 70% for no calibration, which demonstrates a good adaptability with minor calibration. Fig. 3(a) is calculated by randomly choosing 80% of the samples as training data and using the rest 20% to test the accuracy and loss. Fig. 3(b) is repeating the process mentioned above only for the data from a specific number of beacons. Fig. 3(c) shows that 200 samples for each activity (total 1000) from a female and a male were used as the base training data, while 20 samples were measured for each activity for every new user while specific numbers of them are randomly chosen as the calibration data (additional training data) and the rest are used as the test data. Similarly, Fig. 3(d) shows that 50 samples for each activity in a children room and a conference room were measured, among which a specific number of data were randomly chosen along with all the data from the other rooms to train the model while the rest data in this room was used to test the accuracy.

Table 2 shows how likely one activity can be identified as each activity. ''Stand'' and ''sit'' have the highest confusion rate because the sensor on the lap is less sensitive due to the larger distance to the receiver on the head and because both activities feature virtually no change in the upper body as it is essentially hard to detect a ''no change''. Compared to other works using RF signal for HAR [42], [43], this paper is the first realization using a truly wireless system with miniaturized antennas that demonstrates a high accuracy to detect and identify a variety of individual activities and an excellent adaptability to different situations. While this method requiring a significantly less amount of information (no need for phase information or multiple frequencies), the accuracy is still very high and comparable to or even better than those using much more information (e.g.87.5/88.3/95.8/75.0% in [42], 97.1/98.8% in [43]). Even when comparing with other wearable sensors

TABLE 2. Confusion matrix of HAR with average values (%) and standard deviations in brackets.

		Probability of human activity classification (%)				
		stand	right jab	left jab	sit	walk
Actual activity	stand	88.66 (3.89)	1.77 (0.85)	1.35(0.91)	8.12(3.12)	0.1(0.23)
	right jab	2.40(1.32)	91.98(3.14)	1.98(0.98)	2.18(1.64)	1.46(0.67)
	left jab	3.44(1.8)	1.98(0.86)	92.29(2.64)	1.25(1.19)	1.04(0.86)
	sit	5.73(2.53)	0.94(0.63)	0.73(0.61)	92.6(2.67)	0(0)
	walk	0.21(0.32)	3.02(1.41)	2.81(2.20)	0(0)	93.96(2.39)

(e.g. accelerometers) systems which shows accuracy ranging from 56% to 98% in [27], the proposed approach show a better or comparable accuracy.

IV. CONCLUSION

This paper provides an overview of wearable antennas for on-body networks, from designing an antenna to overcome body effects, flexible antenna fabrication, to an on-body networks application, human activity recognition using RSSI and machine learning. This paper shows a integrated solution to the all three major challenges of wearable antenna design: body effect, minimization, and flexible fabrication, and demonstrates a novel mosaic antenna that outperforms comparing to conventional antennas. Firstly, the wearable antenna for cross-body communication is very important and troublesome due to body effects. Five widely used antennas are compared for their on-body performances to find the best on-body antennas that can overcome the body effects, especially shadowing effect. Based the result of the comparison, a novel wearable antenna, a mosaic antenna that features a low profile (90% height reduction to the monopole antenna), a miniaturized size as small as a tenth of a wavelength, similar operation to the monopole antenna and a maximal surface waves excitation in all directions. Secondly, a flexible mosaic antenna is fabricated with inkjet-printing on PTFE substrate for the first time. This process, due to its additive manufacturing nature, is highly customizable, low-cost, environmentally friendly, and fast. The last but not least, by utilizing the on-body networks which equipped with the antenna that can maximally excite the surface waves, the activity of the body can be detected with an accuracy 91.9% for six beacons, which can be further improved with a larger number of beacons. For new users and new environment, an accuracy more than 85% can be achieved which can be improved if more calibration data collected for new users and new locations.

REFERENCES

[1] Kenry, J. C. Yeo, and C. T. Lim, "Emerging flexible and wearable physical sensing platforms for healthcare and biomedical applications," *Microsyst. Nanoeng.*, vol. 2, no. 1, p. 16043, Dec. 2016.

[2] X. Huang, T. Leng, M. Zhu, X. Zhang, J. Chen, K. Chang, M. Aqeeli, A. K. Geim, K. S. Novoselov, and Z. Hu, "Highly flexible and conductive printed graphene for wireless wearable communications applications," *Sci. Rep.*, vol. 5, no. 1, Nov. 2015, Art. no. 18298.

[3] M. F. Farooqui and A. Shamim, "Low cost inkjet printed smart bandage for wireless monitoring of chronic wounds," *Sci. Rep.*, vol. 6, Jun. 2016, Art. no. 28949.

[4] Y. Hao and R. Foster, "Wireless body sensor networks for health-monitoring applications," *Physiol. Meas.*, vol. 29, no. 11, pp. R27–R56, Nov. 2008.

[5] Z. Chen, J. Xi, W. Huang, and M. M. F. Yuen, "Stretchable conductive elastomer for wireless wearable communication applications," *Sci. Rep.*, vol. 7, no. 1, Dec. 2017, Art. no. 10958.

[6] A. Rahman, M. T. Islam, M. J. Singh, S. Kibria, and M. Akhtaruzzaman, "Electromagnetic performances analysis of an ultra-wideband and flexible material antenna in microwave breast imaging: To implement a wearable medical bra," *Sci. Rep.*, vol. 6, no. 1, Dec. 2016, Art. no. 38906.

[7] Federal Communications Commission. *Body Tissue Dielectric Parameters*. Accessed: Apr. 27, 2018. [Online]. Available: https://www.fcc.gov/general/body-tissue-dielectric-parameters

[8] C. Gabriel, S. Gabriel, and E. Corthout, "The dielectric properties of biological tissues: I. Literature survey," *Phys. Med. Biol.*, vol. 41, no. 11, pp. 2231–2249, Nov. 1996.

[9] L. Akhoondzadeh-Asl, Y. Nechayev, and P. S. Hall, "Surface and creeping waves excitation by body-worn antennas," in *Proc. Loughborough Antennas Propag. Conf.*, Nov. 2010, pp. 48–51.

[10] T. Alves, B. Poussot, and J.-M. Laheurte, "Analytical propagation modeling of BAN channels based on the creeping-wave theory," *IEEE Trans. Antennas Propag.*, vol. 59, no. 4, pp. 1269–1274, Apr. 2011.

[11] P. S. Hall, Y. Hao, Y. I. Nechayev, A. Alomainy, C. C. Constantinou, C. Parini, M. R. Kamarudin, T. Z. Salim, D. T. Hee, and R. Dubrovka, "Antennas and propagation for on-body communication systems," *IEEE Antennas Propag. Mag.*, vol. 49, no. 3, pp. 41–58, 2007.

[12] G. A. Conway and W. G. Scanlon, "Antennas for over-body-surface communication at 2.45 GHz," *IEEE Trans. Antennas Propag.*, vol. 57, no. 4, pp. 844–855, Apr. 2009.

[13] R. Khouri, P. Ratajczak, P. Brachat, and R. Staraj, "A thin surface-wave antenna using a via-less EBG structure for 2.45 GHz on-body communication systems," in *Proc. 4th Eur. Conf. Antennas Propag. (EuCAP)*, Apr. 2010, pp. 1–4.

[14] Z. H. Jiang, D. E. Brocker, P. E. Sieber, and D. H. Werner, "A compact, low-profile metasurface-enabled antenna for wearable medical body-area network devices," *IEEE Trans. Antennas Propag.*, vol. 62, no. 8, pp. 4021–4030, Aug. 2014.

[15] S. Yan, P. J. Soh, and G. A. E. Vandenbosch, "Compact all-textile dual-band antenna loaded with metamaterial-inspired structure," *IEEE Antennas Wireless Propag. Lett.*, vol. 14, pp. 1486–1489, 2015.

[16] S. Yan and G. A. E. Vandenbosch, "Radiation pattern-reconfigurable wearable antenna based on metamaterial structure," *IEEE Antennas Wireless Propag. Lett.*, vol. 15, pp. 1715–1718, 2016.

[17] H. Khaleel, *Innovation in Wearable and Flexible Antennas*. Southampton, U.K.: WIT Press, 2014.

[18] R. Salvado, C. Loss, R. Gonçalves, and P. Pinho, "Textile materials for the design of wearable antennas: A survey," *Sensors*, vol. 12, no. 11, pp. 15841–15857, 2012.

[19] M. Stoppa and A. Chiolerio, "Wearable electronics and smart textiles: A critical review," *Sensors*, vol. 14, no. 7, pp. 11957–11992, 2014.

[20] A. Tsolis, W. Whittow, A. Alexandridis, and J. Vardaxoglou, "Embroidery and related manufacturing techniques for wearable antennas: Challenges and opportunities," *Electronics*, vol. 3, no. 2, pp. 314–338, 2014.

[21] R. B. V. B. Simorangkir, Y. Yang, K. P. Esselle, and Y. Diao, "A varactor-tuned frequency-reconfigurable fabric antenna embedded in polymer: Assessment of suitability for wearable applications," in *IEEE MTT-S Int. Microw. Symp. Dig.*, Jun. 2017, pp. 204–207.

[22] G. J. Hayes, J.-H. So, A. Qusba, M. D. Dickey, and G. Lazzi, "Flexible liquid metal alloy (EGaIn) microstrip patch antenna," *IEEE Trans. Antennas Propag.*, vol. 60, no. 5, pp. 2151–2156, May 2012.

[23] S. Yang, P. Liu, M. Yang, Q. Wang, J. Song, and L. Dong, "From flexible and stretchable meta-atom to metamaterial: A wearable microwave metaskin with tunable frequency selective and cloaking effects," *Sci. Rep.*, vol. 6, no. 1, Apr. 2016, Art. no. 21921.

[24] J. Kim, M. Kim, M.-S. Lee, K. Kim, S. Ji, Y.-T. Kim, J. Park, K. Na, K.-H. Bae, H. Kyun Kim, F. Bien, C. Young Lee, and J.-U. Park, "Wearable smart sensor systems integrated on soft contact lenses for wireless ocular diagnostics," *Nature Commun.*, vol. 8, no. 1, p. 14997, Apr. 2017.

[25] J. G. Hester, S. Kim, J. Bito, T. Le, J. Kimionis, D. Revier, C. Saintsing, W. Su, B. Tehrani, A. Traille, B. S. Cook, and M. M. Tentzeris, "Additively manufactured nanotechnology and origami-enabled flexible microwave electronics," *Proc. IEEE*, vol. 103, no. 4, pp. 583–606, Apr. 2015.

[26] J. Bito, R. Bahr, J. Hester, J. Kimionis, A. Nauroze, W. Su, B. Tehrani, and M. M. Tentzeris, "Inkjet-/3D-/4D-printed autonomous wearable RF modules for biomonitoring, positioning and sensing applications," *Proc. SPIE*, vol. 10194, 2017, Art. no. 101940Z.

[27] O. D. Lara and M. A. Labrador, "A survey on human activity recognition using wearable sensors," *IEEE Commun. Surveys Tuts.*, vol. 15, no. 3, pp. 1192–1209, 3rd Quart., 2013.

[28] J. Zhu and G. V. Eleftheriades, "A compact transmission-line metamaterial antenna with extended bandwidth," *IEEE Antennas Wireless Propag. Lett.*, vol. 8, pp. 295–298, 2009.

[29] J. Zhu, M. A. Antoniades, and G. V. Eleftheriades, "A compact tri-band monopole antenna with single-cell metamaterial loading," *IEEE Trans. Antennas Propag.*, vol. 58, no. 4, pp. 1031–1038, Apr. 2010.

[30] J. Zhu and G. V. Eleftheriades, "Dual-band metamaterial-inspired small monopole antenna for WiFi applications," *Electron. Lett.*, vol. 45, no. 22, pp. 1104–1106, 2009.

[31] M. A. Antoniades and G. V. Eleftheriades, "A folded-monopole model for electrically small NRI-TL metamaterial antennas," *IEEE Antennas Wireless Propag. Lett.*, vol. 7, pp. 425–428, 2008.

[32] S. Kim, M. Bozzi, M. M. Tentzeris, V. Lakafosis, T. Le, R. Vyas, A. Georgiadis, J. Cooper, B. Cook, R. Moro, A. Collado, and H. Lee, "Inkjet-printed antennas, sensors and circuits on paper substrate," *IET Microw., Antennas Propag.*, vol. 7, no. 10, pp. 858–868, Jul. 2013.

[33] Y. Y. Lim, Y. M. Goh, and C. Liu, "Surface treatments for inkjet printing onto a PTFE-based substrate for high frequency applications," *Ind. Eng. Chem. Res.*, vol. 52, no. 33, pp. 11564–11574, Aug. 2013.

[34] S. R. Kim, "Surface modification of poly (tetrafluoroethylene) film by chemical etching, plasma, and ion beam treatments," *J. Appl. Polym. Sci.*, vol. 77, no. 9, pp. 1913–1920, 2000.

[35] A. Graves, A.-R. Mohamed, and G. Hinton, "Speech recognition with deep recurrent neural networks," in *Proc. IEEE Int. Conf. Acoust., Speech Signal Process.*, May 2013, pp. 6645–6649.

[36] L. Yao, A. Torabi, K. Cho, N. Ballas, C. Pal, H. Larochelle, and A. Courville, "Describing videos by exploiting temporal structure," in *Proc. IEEE Int. Conf. Comput. Vis. (ICCV)*, Dec. 2015, pp. 4507–4515.

[37] K. Kawakami, "Supervised sequence labelling with recurrent neural networks," Ph.D. dissertation, Tech. Univ. Munich, Munich, Germany, 2008.

[38] S. Ma, L. Sigal, and S. Sclaroff, "Learning activity progression in LSTMs for activity detection and early detection," in *Proc. IEEE Conf. Comput. Vis. Pattern Recognit. (CVPR)*, Jun. 2016, pp. 1942–1950.

[39] Y. Chen, K. Zhong, J. Zhang, Q. Sun, and X. Zhao, "LSTM networks for mobile human activity recognition," in *Proc. Int. Conf. Artif. Intell., Technol. Appl. (ICAITA)*, 2016, pp. 50–53.

[40] A. Murad and J.-Y. Pyun, "Deep recurrent neural networks for human activity recognition," *Sensors*, vol. 17, no. 11, p. 2556, 2017.

[41] T. Plötz, N. Y. Hammerla, and P. Olivier, "Feature learning for activity recognition in ubiquitous computing," in *Proc. Int. Joint Conf. Artif. Intell. (IJCAI)*, 2011, vol. 22, no. 1, p. 1729.

[42] Y. Li, D. Xue, E. Forrister, G. Lee, B. Garner, and Y. Kim, "Human activity classification based on dynamic time warping of an on-body creeping wave signal," *IEEE Trans. Antennas Propag.*, vol. 64, no. 11, pp. 4901–4905, Nov. 2016.

[43] Y. Kim and Y. Li, "Human activity classification with transmission and reflection coefficients of on-body antennas through deep convolutional neural networks," *IEEE Trans. Antennas Propag.*, vol. 65, no. 5, pp. 2764–2768, May 2017.

WENJING SU (Member, IEEE) received the B.S. degree in electrical engineering from the Beijing Institute of Technology, Beijing, China, in 2013, and the Ph.D. degree in electrical and computer engineering from the Georgia Institute of Technology, Atlanta, GA, USA, in 2018.

In fall 2013, she joined Agile Technologies for High-Performance Electromagnetic Novel Applications (ATHENA) Research Group, led by Dr. M. M. Tentzeris. She is currently working at Google. She has authored over 37 articles in refereed journals and conference proceedings and holds four patents/patent applications. Her research interfaces advance novel fabrication technique (e.g., inkjet-printing, 3D printing), special mechanical structures (e.g., microfluidics, origami), and microwave components/antennas to solve problems in smart health, wearable electronics in the Internet-of-Things (IoT) applications. Her research interests include wearable antennas, flexible electronics, applied electromagnetics, additively manufactured electronics, wireless sensing, machine-learning aid sensing, green electronics, RFID, and reconfigurable antennas.

JIANG ZHU (Senior Member, IEEE) received the B.S. degree from Zhejiang University, China, in 2003, the M.A.Sc. degree from McMaster University, Canada, in 2006, and the Ph.D. degree from the University of Toronto, Canada, in 2010, all in electrical engineering. From 2010 to 2014, he was a Senior Hardware Engineer with Apple Inc., Cupertino, CA, USA. From 2014 to 2016, he was with Google[x] Life Science, and then Verily Life Science, a subsidiary of Alphabet Inc. He is currently with Google LLC, Mountain View, CA, USA, as the Engineering Manager of Wireless Hardware Group for Emerging Wearables, Virtual Reality and Augmented Reality Technologies and Projects. He has published scientific results in *Physical Review Letters*, the IEEE TRANSACTIONS ON ANTENNAS AND PROPAGATION, the IEEE TRANSACTIONS ON MICROWAVE THEORY AND TECHNIQUES, IEEE ACCESS, the IEEE ANTENNAS AND WIRELESS PROPAGATION LETTERS, *IET Microwaves*, *Antennas Propagation*, and *Electronic Letters*. He holds over 50 granted/filed U.S. patents. His research interests include antennas, wearables, the Internet-of-Things, and wireless sensing.

Dr. Zhu is a member of the IEEE AP-S Industrial Initiatives and Listings Committee and a member of the IEEE MTT-26 RFID, Wireless Sensors, and IoT Committee. He serves on TPC and TPRC for numerous conferences, including IEEE APS, IMS, and RWS. He was a recipient of the IEEE Microwave Theory and Techniques Society Outstanding Young Engineer Award in 2020 and the IEEE Antennas and Propagation Society Doctoral Research Award, in 2009. He has been an Associate Editor of the IEEE INTERNET OF THINGS JOURNAL, the IEEE TRANSACTIONS ON ANTENNAS AND PROPAGATION, the IEEE ANTENNAS AND WIRELESS PROPAGATION LETTERS, and *IET Microwaves, Antennas, and Propagation*.

HUAN LIAO received the B.S. degree in electrical engineering from the University of Science and Technology of China, in 2006, and the Ph.D. degree in electrical engineering from the University of California at Davis, Davis, CA, USA, in 2013. She joined Google Inc., in 2012, and has been working on the antenna and RF design on various consumer hardware products.

MANOS M. TENTZERIS (Fellow, IEEE) received the Diploma degree *(magna cum laude)* in electrical and computer engineering from the National Technical University of Athens, Athens, Greece, and the M.S. and Ph.D. degrees in electrical engineering and computer science from the University of Michigan, Ann Arbor, MI, USA.

He is currently a Ken Byers Professor in flexible electronics with the School of Electrical and Computer Engineering, Georgia Institute of Technology, Atlanta, GA, USA, where he heads the ATHENA Research Group (20 researchers). He served as the Head of the GTECE Electromagnetics Technical Interest Group, the Georgia Electronic Design Center Associate Director of RFID/Sensors Research, the Georgia Institute of Technology NSF-Packaging Research Center Associate Director of RF Research, and the RF Alliance Leader. He has helped to develop academic programs in 3-D/inkjet-printed RF electronics and modules, flexible electronics, origami and morphing electromagnetics, highly integrated/multilayer packaging for RF and wireless applications using ceramic and organic flexible materials, paper-based RFID's and sensors, wireless sensors and biosensors, wearable electronics, ''Green'' electronics, energy harvesting and wireless power transfer, nanotechnology applications in RF, microwave MEMs, and SOP-integrated (UWB, multiband, mmW, and conformal) antennas. He has authored more than 650 articles in refereed journals and conference proceedings, five books, and 25 book chapters. He was a Visiting Professor with the Technical University of Munich, Munich, Germany, in 2002, with GTRI-Ireland, Athlone, Ireland, in 2009, and with LAAS-CNRS, Toulouse, France, in 2010.

Dr. Tentzeris is a member of the URSI-Commission D and the MTT-15 Committee, an Associate Member of the European Microwave Association (EuMA), a Fellow of the Electromagnetic Academy, and a member of the Technical Chamber of Greece. He served as one of the IEEE MTT-S Distinguished Microwave Lecturers from 2010 to 2012 and is one of the IEEE CRFID Distinguished Lecturers. He has given more than 100 invited talks to various universities and companies all over the world. He was a recipient/co-recipient of the 2019 Humboldt Research Prize, the 2017 Georgia Institute of Technology Outstanding Achievement in Research Program Development Award, the 2016 Bell Labs Award Competition Third Prize, the 2015 *IET Microwaves, Antennas, and Propagation* Premium Award, the 2014 Georgia Institute of Technology ECE Distinguished Faculty Achievement Award, the 2014 IEEE RFID-TA Best Student Paper Award, the 2013 *IET Microwaves, Antennas, and Propagation* Premium Award, the 2012 FiDiPro Award in Finland, the iCMG Architecture Award of Excellence, the 2010 IEEE Antennas and Propagation Society Piergiorgio L. E. Uslenghi Letters Prize Paper Award, the 2011 International Workshop on Structural Health Monitoring Best Student Paper Award, the 2010 Georgia Institute of Technology Senior Faculty Outstanding Undergraduate Research Mentor Award, the 2009 IEEE Transactions on Components and Packaging Technologies Best Paper Award, the 2009 E. T. S. Walton Award from the Irish Science Foundation, the 2007 IEEE AP-S Symposium Best Student Paper Award, the 2007 IEEE MTT-S IMS Third Best Student Paper Award, the 2007 ISAP 2007 Poster Presentation Award, the 2006 IEEE MTT-S Outstanding Young Engineer Award, the 2006 Asia–Pacific Microwave Conference Award, the 2004 IEEE Transactions on Advanced Packaging Commendable Paper Award, the 2003 NASA Godfrey ''Art'' Anzic Collaborative Distinguished Publication Award, the 2003 IBC International Educator of the Year Award, the 2003 IEEE CPMT Outstanding Young Engineer Award, the 2002 International Conference on Microwave and Millimeter-Wave Technology Best Paper Award, Beijing, China, the 2002 Georgia Institute of Technology–ECE Outstanding Junior Faculty Award, the 2001 ACES Conference Best Paper Award, the 2000 NSF CAREER Award, and the 1997 Best Paper Award of the International Hybrid Microelectronics and Packaging Society. He was the TPC Chair of the IEEE MTT-S IMS 2008 Symposium and the Chair of the 2005 IEEE CEM-TD Workshop. He is the Vice-Chair of the RF Technical Committee (TC16) of the IEEE CPMT Society. He is the Founder and Chair of the RFID Technical Committee (TC24) of the IEEE MTT-S and the Secretary/Treasurer of the IEEE C-RFID. He is an Associate Editor of the IEEE TRANSACTIONS ON MICROWAVE THEORY AND TECHNIQUES, the IEEE TRANSACTIONS ON ADVANCED PACKAGING, and the *International Journal on Antennas and Propagation*.